BEAM PHYSICS AT TEVATRON COMPLEX[*]

Valeri Lebedev[#], FNAL, Batavia, IL 60510, USA

Abstract

The challenge of achieving the Tevatron Run II luminosity goal of $3 \cdot 10^{32}$ cm^{-2}s^{-1} requires high level of engineering and machine operation, good and reliable diagnostics, and clear understanding of the underlying accelerator physics. Recent history demonstrated steady increase of the Tevatron luminosity, which was supported by each of the three listed above items. This report reviews major developments in the accelerator physics, which contributed in the Run II luminosity growth. Present limitations of the luminosity and projections of further luminosity growth are also discussed.

INTRODUCTION

The commissioning of Tevatron Run II began in the spring of 2001 with the first luminosity seen in June. By the year end the luminosity was in the range of $(5\text{-}10) \cdot 10^{30}$ cm^{-2}s^{-1}. Although the luminosity growth was significantly slower than expected, steady growth of luminosity has been demonstrated during last two years with the peak luminosity of $42 \cdot 10^{30}$ cm^{-2}s^{-1} achieved in April 2003. This luminosity growth would not be possible without deep insight into the accelerator physics problems, which have restricted the machine operation. Important contributions came from (1) optics correction in transfer lines, (2) improvements of helical beam separation in Tevatron [1], (3) introduction of dual lattice operation in Accumulator to suppress intrabeam scattering (IBS), (4) feedforward compensation of beam loading in Main Injector, (5) correction of injection errors for antiproton transfers from MI to Tevatron, (6) understanding transverse instability in Tevatron with subsequent transverse impedance reduction [2], and (7) active damping of instabilities in Tevatron [3,4]. Although understanding of longitudinal undamped oscillations in Tevatron [5] not contribute directly to the luminosity growth it has been critical for planning Run II upgrades. Several interesting accelerator physics problems encountered in Run II commissioning are considered in this report.

1 IBS IN ACCUMULATOR

Accumulator [6] stacks antiprotons with an average accumulation rate of $\sim 10^{11}$ per hour, so that after 20 hours the stack of $\sim 2 \cdot 10^{12}$ antiprotons can be accumulated. The total number of antiprotons along with the longitudinal and transverse emittances are the major parameters which determine the collider luminosity. At the beginning of 2002, once the antiproton source was successfully commissioned, it became clear that there is a strong heating of horizontal degree of freedom in Accumulator. That caused

the horizontal emittance to be significantly higher than in Run I (see Figure 1).

The source of the problem was found to be the upgrade of machine optics, which caused an increase in IBS heating. The optics upgrade was aimed to increase the antiproton production [7]. That required an increase of frequency band for stochastic cooling systems with subsequent decrease of the slip factor η to prevent the bad mixing. Although the betatron tunes were changed insignificantly the IBS heating rate was strongly increased.
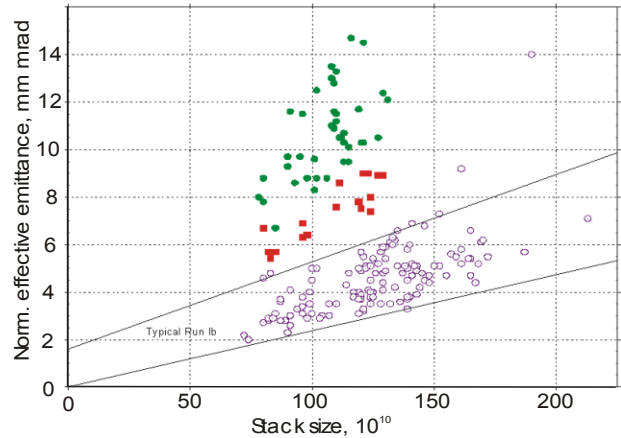

Figure 1: Dependences of antiproton normalized effective emittance, $(\varepsilon_x + \varepsilon_y)/2$, on beam current (100 mA = 10^{12}) before upgrades (●), after the stochastic cooling upgrade (■), and after both the cooling and optics upgrades were implemented (o). Each dot corresponds to one collider shot. Lines present emittance boundaries for Run Ib.

Typically, in Accumulator, the longitudinal velocity spread in the beam frame is much smaller than the transverse ones, and the transverse emittance growth is dominated by excitation of betatron motion due to energy changes at collisions. That significantly simplifies formulas. If $k_{\parallel} = 2.2\sigma_p/(\gamma\theta_{\perp}) \leq 0.15$ the IBS growth rates are:

$$\frac{d}{dt}\begin{bmatrix}\sigma_p^2\\\varepsilon_x\\\varepsilon_y\end{bmatrix} \approx \frac{r_p^2 cN}{4\gamma^3\beta^3 C}\left\langle\frac{\sqrt{2\pi}L_C}{\sigma_x\sigma_y\theta_{\perp}}\begin{bmatrix}2(1-k_{\parallel})\\A_x(1-\kappa)\\A_x\kappa\end{bmatrix}\right\rangle_s . \quad (1)$$

Here r_p and c are the proton classical radius and the speed of light, γ and β are the relativistic factors, C is the ring circumference, N is the number of particles, σ_p is the rms relative momentum spread, σ_x, σ_y, θ_x, and θ_y are the rms sizes and the local angular spreads, κ is the x-y coupling parameter, $\theta_{\perp} = \sqrt{\theta_x^2 + \theta_y^2}$, $\langle\ \rangle_s$ denotes averaging over the ring, L_C is the Coulomb logarithm ($L_C \approx 20$),

$$A_x = \frac{D_x^2 + (D_x'\beta_x + \alpha_x D_x)^2}{\beta_x} , \quad (2)$$

β_x and α_x are the horizontal beta- and alpha-functions, and

D_x and D'_x are the dispersion and its derivative.

Usually ring optics is sufficiently smooth, and the second term in Eq. (2) can be neglected. However, in the case of Accumulator optics upgrade, average value of A_x is well above the value corresponding to the smooth lattice approximation and 2.5 times higher the value before the upgrade. That caused strong amplification of horizontal emittance growth. To reduce the IBS we introduced dual lattice operation. The stacking is performed at the stacking lattice, which has been designed for fast stacking but has strong heating due to IBS. After stacking is completed the machine optics is retuned to the "shot" lattice (similar to the Run I lattice), which has the same tunes but smaller IBS heating, and therefore is more suitable for the final cooling. After about 20 minutes cooling, the beam is ready for extraction.
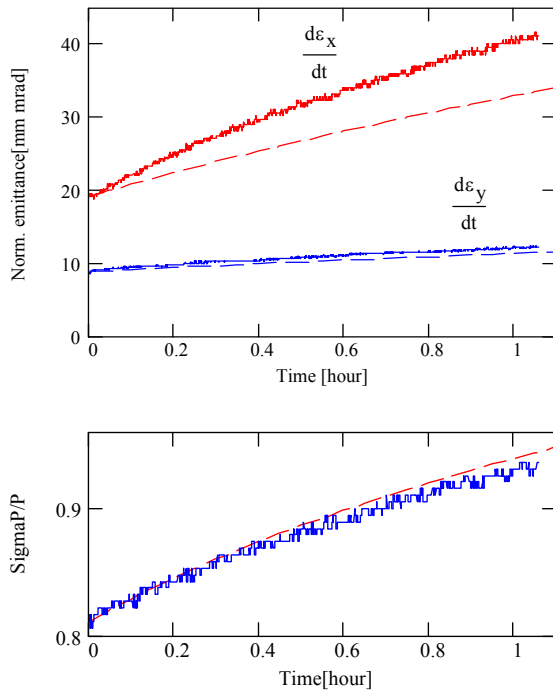

Figure 2: Measured (solid lines) and calculated (dashed lines) normalized 95% emittances (top) and energy spread (bottom) for antiproton current of 105 mA in Accumulator, $\kappa = 0.1$ is used in the simulations.

Figure 2 presents computed and measured emittances of antiproton beam for stacking lattice with cooling turned off. There is good agreement between theory and measurements for the energy spread and the vertical emittance but it is not as good for horizontal emittance. However good agreement was found in the case of proton beam. The difference is caused by additional heating from the self-stabilized two-beam instability due to small amount of ions stored in the beam. The instability appears at antiproton currents above ~30 mA. The emittance growth related to multiple collisions with the residual gas is sufficiently large and was taken into account in the simulations.

The described optics manipulations together with the core cooling upgrade were introduced after the 2002 summer shutdown and allowed us to achieve the antiproton beam emittances required for Run II.

2 SINGLE AND MULTIPLE SCATTERING

There are a few applications in the Tevatron complex for which simultaneous consideration of multiple and single Coulomb scattering is important.

The first one is associated with separation of different heating mechanisms contributing to transverse emittance growth in Tevatron. The three basic sources of the beam heating are IBS, multiple scattering on the residual gas and the noise in magnets, kickers, etc. While the first one can be easily separated due to strong dependence on the beam parameters, the effects of the other two look very similar. Nevertheless, there is a fundamental difference between them. In distinguish from the noise the beam interaction with residual gas, additionally to diffusion, creates non-gaussian tails due to single scattering. Approach developed in Ref. [8] uses an integro-differential equation to describe the evolution of the distribution in a linear focusing field. The equation correctly treats both single and multiple scattering and can be written in the following form

$$\frac{\partial f}{\partial t} - \lambda \frac{\partial}{\partial I}(If) = \int_0^\infty W(I,I')\big(f(I',t) - f(I,t)\big)\mathrm{d}I' \ , \quad (3)$$

where the kernel is

$$W(I,I') = \frac{D\left(I + I' + I_{\min}/2\right)}{L_C\left((I - I')^2 + (I + I')I_{\min} + I_{\min}^2/4\right)^{3/2}} \ , (4)$$

λ is the damping decrement (if cooling is present), D is the diffusion coefficient, $L_C = \ln\left(\sqrt{I_{\max}/I_{\min}}\right)$ is the Coulomb logarithm, $I_{\min}$ and $I_{\max}$ are the minimum and maximum actions.

The following experiment was performed to measure the emittance growth rate and to separate contributions of noise and gas scattering. A low intensity beam was injected into Tevatron. The beam was debunched (to reduce IBS) and scraped in both planes to a known size. The scrapers were then removed, and the beam was left alone for 1 hour. To measure resulting distribution we scraped the beam vertically while measuring the beam current as function of scraper position. Good agreement between the measurements and numerical solution of Eq. (3) ($\lambda = 0$) has been found. Both the emittance growth in the core (5 mm mrad/hour) and the tail population were described well by the model. That means that in the case of small intensity beam, when IBS is negligible, gas scattering is a major source of the beam heating and there is no visible heating could be associated with noise. Last year vacuum improvements yielded some reduction of the beam heating due to gas scattering and reduced background in CDF and D0 detectors.

The second example is related to the beam lifetime computations in Recycler where the beam emittances and machine acceptances are quite close. Solving Eq. (3) with

zero boundary condition at the machine acceptance we found the dependence of the rms beam size and the beam lifetime as functions of time for different cooling decrements. After some time the system comes into equilibrium, where the shape of distribution function does not depend on time, and the intensity decays exponentially with the decay time τ_∞. We define the lifetime correction factor, K, as a ratio of τ_∞ at given equilibrium emittance (determined by cooling decrement) to the lifetime of zero-emittance beam (determined by the single scattering only). Figure 3 presents K as a function of ratio of the rms equilibrium emittance to the machine acceptance. Without cooling the rms beam emittance reaches its maximum of ≈ 0.391, where the lifetime is ≈ 40 times worse than for a point-like beam. Although, the model described above was developed for a one-dimensional case, when the aperture is limited in one plane only, the results presented in Figure 3 can be used for the lifetime correction factor of two-dimensional case if the emittances and the acceptances in both planes are equal.
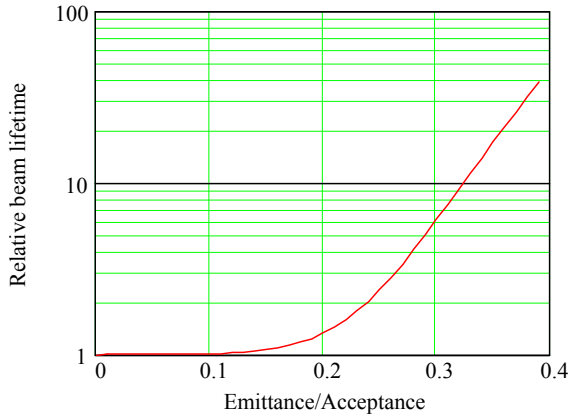

Figure 3: Dependence of the lifetime correction factor, K, on the ratio of the rms emittance to the machine acceptance.

The last example of this section is related to the evolution of longitudinal distribution in Tevatron governed by IBS. In this case the non-linearity of potential well changes the kernel in Eq. (3) to [9]:

$$\widetilde{W}(E,E') = \frac{B\omega_0\omega\omega'}{(E-E')^2}\begin{cases} \dfrac{1}{2\omega} + \dfrac{I}{E'-E} & , \quad E' \geq E + \delta E , \\[2mm] \dfrac{1}{2\omega'} + \dfrac{I'}{E-E'} & , \quad E' \leq E - \delta E . \end{cases} \quad (5)$$

Here ω_0 is the frequency of small amplitude motion, E is the energy, $I = (1/2\pi)\oint p\,dx$ and $\omega = \partial E/\partial I$ are the action and the frequency. Similar to Eq. (4) the divergence in Eq. (5) at $E \approx E'$ need to be confined for the energy difference below $\delta E \sim \omega_0 I_{min}$. Eq. (5) reduces to Eq. (4) for linear motion. For the sinusoidal potential of longitudinal motion the energy is,

$$E = p^2/2 + \omega_0^2 (1 - \cos(x)) \quad . \quad (6)$$

Evolution of the longitudinal bunch profile in time obtained by numerical solution of Eq. (3) with kernel of Eq.

(5) is presented in Figure 4. The initial distribution function has no tails, because before acceleration the particle distribution fits into 4 eV s bucket size, while after acceleration the bucket size is 10 eV s. Therefore the initial particle loss occurs due to the single scattering only, later, however, the tail population grows and diffusion loss begins to dominate. In distinguish from the standard (local) diffusion the large non-gaussian tails are created from the very beginning. For a point-like beam the lifetime is determined by single scattering and is equal to $\tau_0 = 4L_C / D$. The lifetime decreases with beam expansion and, when the beam size achieves its maximum rms size of ≈ 0.931 rad, the lifetime reaches its asymptotic value of $\tau_0 \approx 0.741/D$.
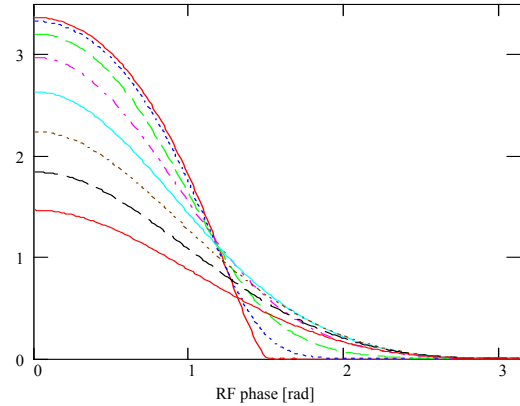

Figure 4: Numerical simulation of the longitudinal bunch profile evolution during the store in Tevatron.

3 LUMINOSITY EVOLUTION

Numerous factors affect the Tevatron luminosity and its evolution in time. Each store is different and because of finite instrumentation accuracy it is practically impossible to state what was different or what came wrong for every particular store. Nevertheless the luminosity evolution is similar for most of the stores. It is driven by some basic processes, which are not very sensitive to the details of distribution function, and therefore the luminosity evolution can be described by comparatively simple parametric model. The model takes into account the major beam heating and particle loss mechanisms. They are (1) the emittance growth and the particle loss due to scattering on the residual gas, (2) the particle loss and the emittance growth due to scattering in IPs, (3) the transverse and longitudinal emittance growth due to IBS, (4) the bunch lengthening due to RF noise, and (5) the particle loss from the bucket due to heating of longitudinal degree of freedom [10]. If the collider tunes are correctly set and the beam intensity is not too high the beam-beam effects are not very important and the model describes the observed dynamics of beam parameters and the luminosity comparatively well.

Figure 5 presents measured and computed luminosity for the Store 2138 (Jan.05.2003). The only free parameters used in the model were the residual gas pressure of

$1.2 \cdot 10^{-9}$ Torr of molecular nitrogen equivalent at room temperature, the x-y coupling parameter $\kappa = 0.45$, and the spectral density of RF phase noise of 50 μrad^2/Hz. They correspond to the gas scattering lifetime of 380 hours, and the bunch lengthening due to RF noise of $2.2 \cdot 10^{-3}$ rad^2/hour. RF phase noise was measured directly [11] and agrees with the fit to the model within the measurement accuracy (factor of 2). The computed proton and antiproton intensities are close to the measured ones as can be seen in Figure 6. It has been critical to use the described above model for non-local diffusion in longitudinal direction to achieve such a good agreement
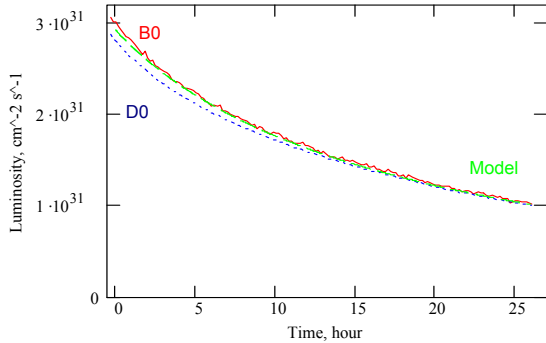

Figure 5: Dependence of luminosity on time for Store 2138; solid and dotted lines - luminosity measured by CDF and D0 detectors, dashed line – model prediction.
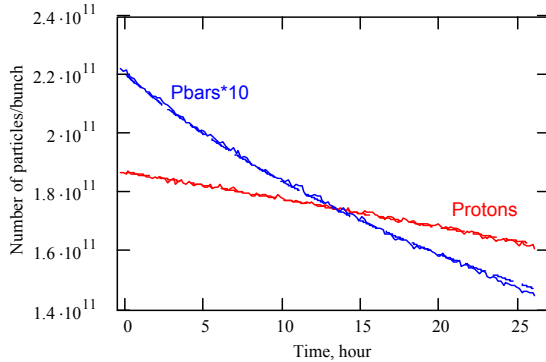

Figure 6: Dependence of intensities for proton and antiproton beams on time for Store 2138; solid lines – measurements, dashed lines - model prediction.
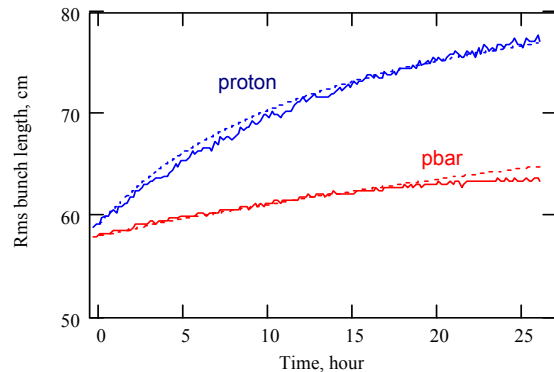

Figure 7: Dependence of bunch lengths for proton and antiproton beams on time for Store 2138; solid lines – measurements, dashed lines - model prediction.

The major mechanism for loss of antiprotons is the luminosity loss. The cross-section of 70 mbarn is used for proton-antiproton scattering in the IP. The proton bunch lengthening (see Figure 7) is mainly driven by IBS, while for low intensity antiproton beam the RF phase noise usually dominates. Figure 8 presents a comparison of measured and computed antiproton emittances versus time. The emittances were measured with synchrotron light monitors [12]. The obtained values were corrected for diffraction to match them with the effective emittance computed from the luminosity and the emittance measurements performed with flying wires at the beginning and the end of the store. At the beginning of the store, the vertical emittance grows significantly faster than the model prediction. Our present belief is that it is related to an amplification of diffusion by the beam-beam effects.
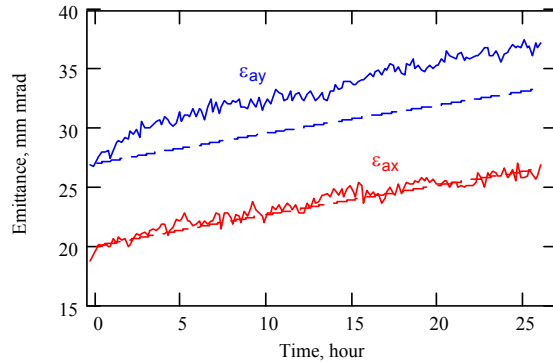

Figure 8: Dependence of horizontal and vertical antiproton beam emittances on time for Store 2138; solid lines – measurements, dashed lines - model prediction.

The store 2138 discussed above has moderate discrepancies with the model, and can be considered a regular store. Most of our stores are influenced more by the beam-beam interaction, but fortunately it weakly affects the luminosity decay and the luminosity integral. Figures 9 and 10 present measured and computed parameters for Store 2328 (Mar.20.2003). The same vacuum and RF phase noise were used in the model. Unlike Store 2138, both the proton and antiproton beam intensities decay faster and the proton bunch length grows significantly slower than the model predicts [12,13]. The most probable cause of such misbehavior is small, uncontrolled store-to-store tune variation causing a loss of dynamic stability for particles at large synchrotron amplitudes with subsequent particle loss and reduction of bunch lengthening.

The results presented above show that the beam-beam interactions certainly affect the luminosity decay. However this effect is sufficiently small. Thus, the developed model, with some reservations, can be used to analyze the luminosity dynamics for the final Run II parameters. Table 1 presents parameters for one of our best stores (Store 2328), typical collider parameters in April 2003 and projections for the final Run II parameters. Evidently, in order to increase the luminosity by a factor of 7.2 times we need to quadruple the number of antiprotons extracted from the stack. The remaining factor of 1.8 should result from the improvements in the antiproton transport and

Tevatron. Three major contributions are an increase of the proton intensity by ~30%, an improvement of coalescing in MI, and improvements of antiproton transport efficiency (from the antiproton stack to the collisions in Tevatron). Two last items are expected to increase the transfer efficiency from ~60% to ~80%. The chosen proton intensity, $2.7 \cdot 10^{11}$ per bunch, corresponds to the linear head-on tune shift of 0.01 for each of two IPs. This is the maximum tune shift achieved in Run Ib with 6×6 bunch operation. We choose the maximum antiproton intensity to be half of the proton intensity. Further increase of antiproton intensity is limited by antiproton production.
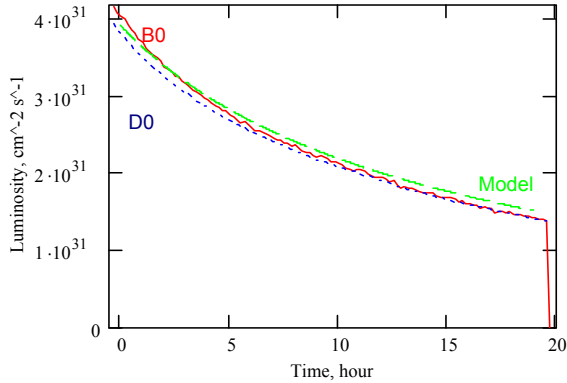

Figure 9: Dependence of luminosity on time for Store 2328; solid and dotted lines - luminosity measured by CDF and D0 detectors, dashed line – model prediction.
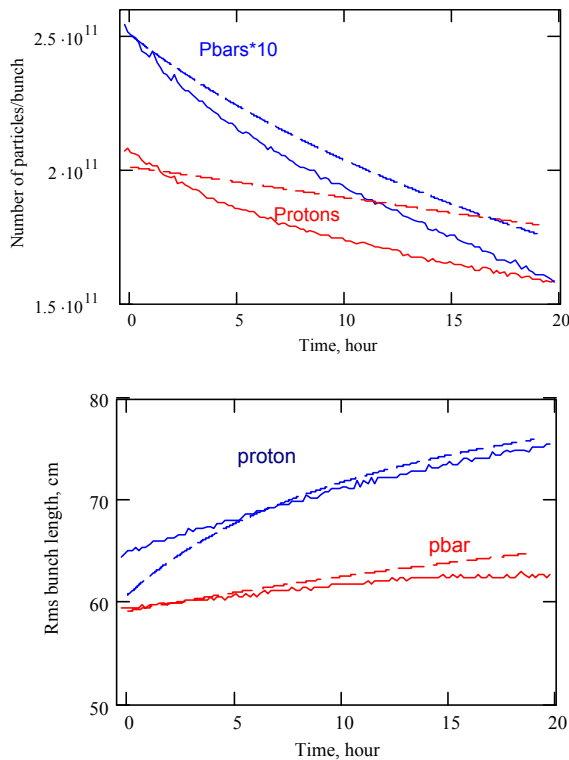

Figure 10: Dependence of intensities (top) and bunch lengths (bottom) for proton and antiproton beams on time for Store 2328; solid lines – measurements, dashed lines - model prediction.

Due to reduction of luminosity lifetime with growth of peak luminosity, the average luminosity grows slower than the peak luminosity. After all Run II upgrades are introduced the luminosity integral is estimated to be ~2.5 fb^{-1}/year.

Table 1: Present and final Run II parameters

	Store 2328	Typical Apr.03	Final Run II
Protons, 10^{10} / bunch	20.7	20	27
Pbars, 10^{10}/ bunch	2.54	2.2	13.5
Norm. 95% proton emittances, $\varepsilon_x/\varepsilon_y$, mm mrad	~14/24	~15/25	20/20
Norm. 95% pbar emittances, $\varepsilon_x/\varepsilon_y$, mm mrad	~15/24	~16/25	20/20
Proton bunch length, cm	65	62	50
Pbar bunch length, cm	59	58	50
Initial luminosity, 10^{30} cm^{-2}s^{-1}	40.5	35	290
Initial luminosity lifetime, hour	11	12	7.1
Store duration, hour	19	20	15.2
Lumin. integral per store, pb^{-1}	1.71	1.2	8.65

REFERENCES

[1] Yu. Alexahin et al.., "Tevatron Lattice Upgrades," these proceedings.

[2] P. Ivanov et al., "Head-Tail Instability at Tevatron," these proceedings.

[3] C.Y. Tan, J. Steimel, "The Tevatron Bunch by Bunch Longitudinal Dampers," these proceedings.

[4] C. Y. Tan, J. Steimel, "The Tevatron Coupled Bunch Mode Transverse Dampers," these proceedings.

[5] R. Moore et al., "Longitudinal Bunch Dynamics in the Tevatron," these proceedings.

[6] J. Peoples, "Antiproton source", Physics of particle accelerators - AIP conf. Proc. 184, 1988, p.1846.

[7] Run II handbook, FNAL, 1998.

[8] V. Lebedev and S. Nagaitsev, Proc. of EPAC 2002, Paris, France, June 4-10, 2002. p. 1362-1364.

[9] A. Burov, Private communications, 2003.

[10] FNAL report for the summer 2003 DoE review, FNAL, 2003.

[11] J. Steimel et al., "Effects of RF noise on the longitudinal emit. growth in Tevatron," these proceedings.

[12] H.W.K.Cheung et al., "Performance of a Beam Monitor in the Fermilab Tevatron Using Synchrotron Light," these proceedings.

[13] A. Tollestrup et al., "Measurements of the longitudinal and transverse beam loss at the Tevatron," these proceedings.

[14] P. Lebrun et al., "Observations on the Luminosity Lifetimes, emittance growth factors and Intra-Beam Scattering at the Tevatron," these proceedings.